Electronic Supplementary Material (ESI) for Physical Chemistry Chemical Physics.

Supporting Information

Laser power and high-temperature dependent Raman study of layered bismuth and copper-based oxytellurides for optoelectronic applications

Prabhukrupa C. Kumar[1], Subrata Senapati[1], Monalisa Pradhan[2], Gopal K. Pradhan[2], Ramakanta Naik[1*]*

[1] Department of Engineering and Materials Physics, Institute of Chemical Technology-Indian Oil Odisha Campus, Bhubaneswar, 751013, India

[2] Department of Physics, School of Applied Science, KIIT Deemed to be University, Bhubaneswar, 751024, India

*Email: subrata.uu@gmail.com

ramakanta.naik@gmail.com

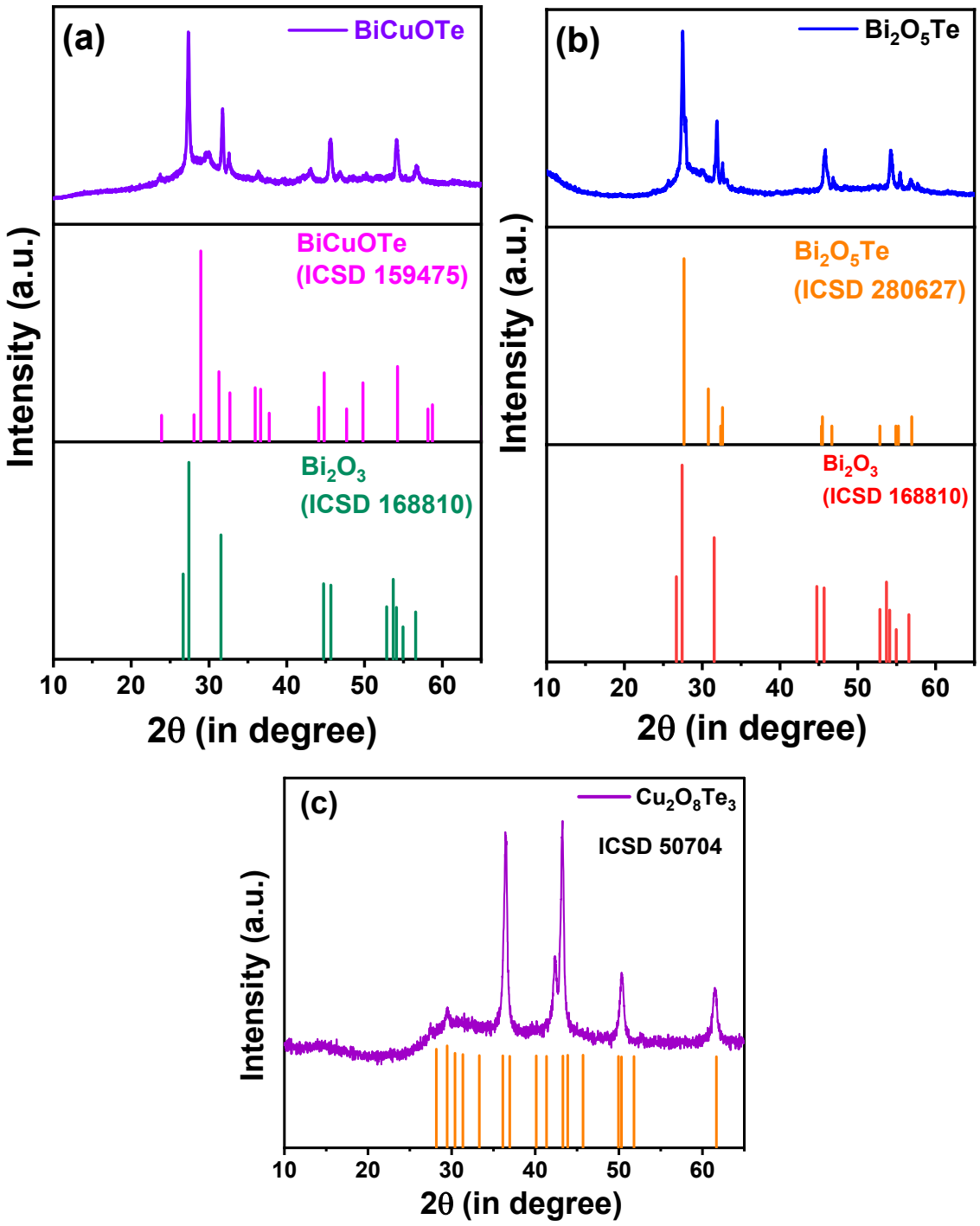

Fig. S1 XRD pattern with the respective matched ICSD cards for (a) BiCuOTe, (b) Bi_2O_5Te and (c) $Cu_2O_8Te_3$ samples.

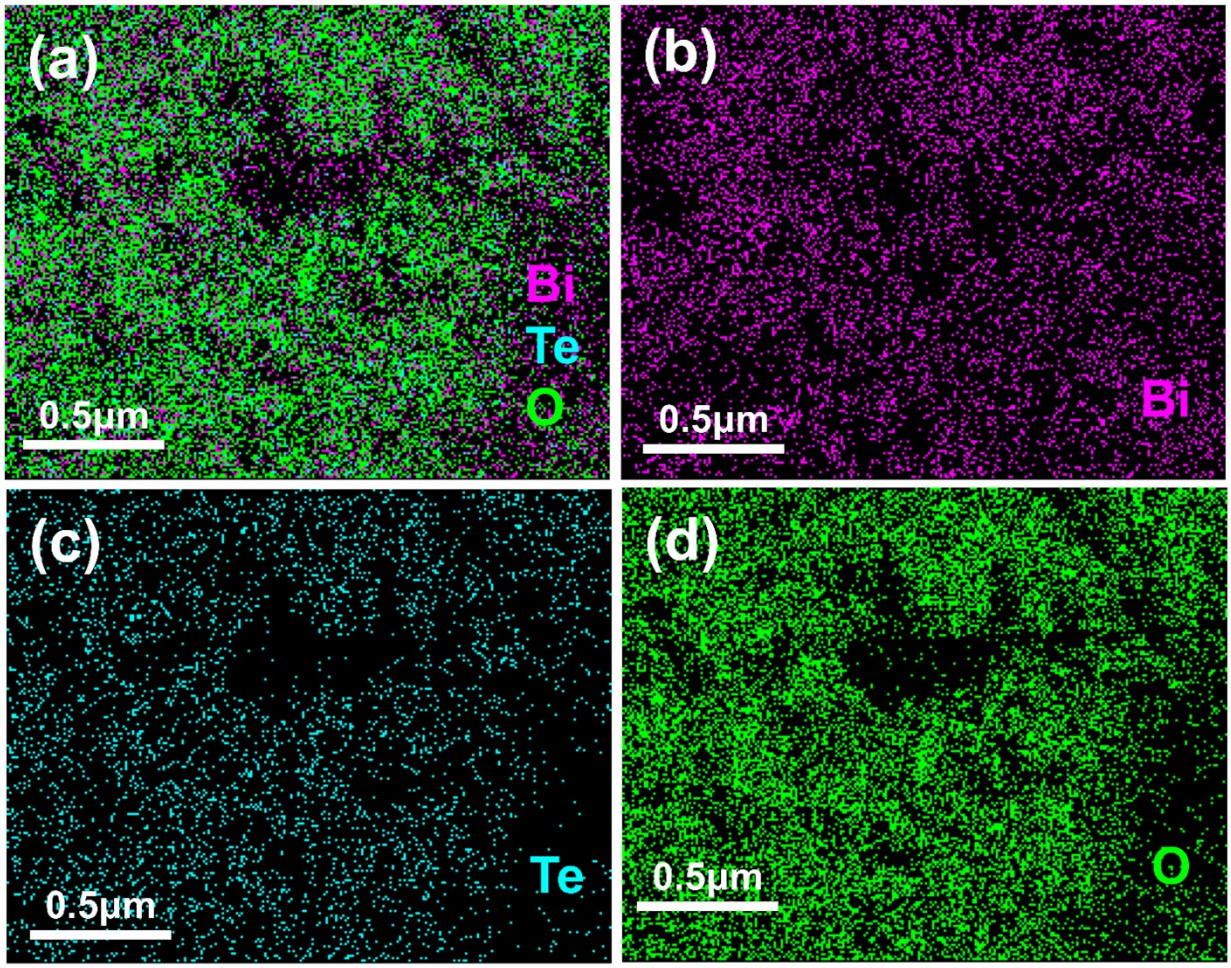

Fig. S2 (a) Combined elemental mapping of the Bi_2O_5Te nanosheets and (b-d) elemental mapping of the individual Bi, O, and Te elements.

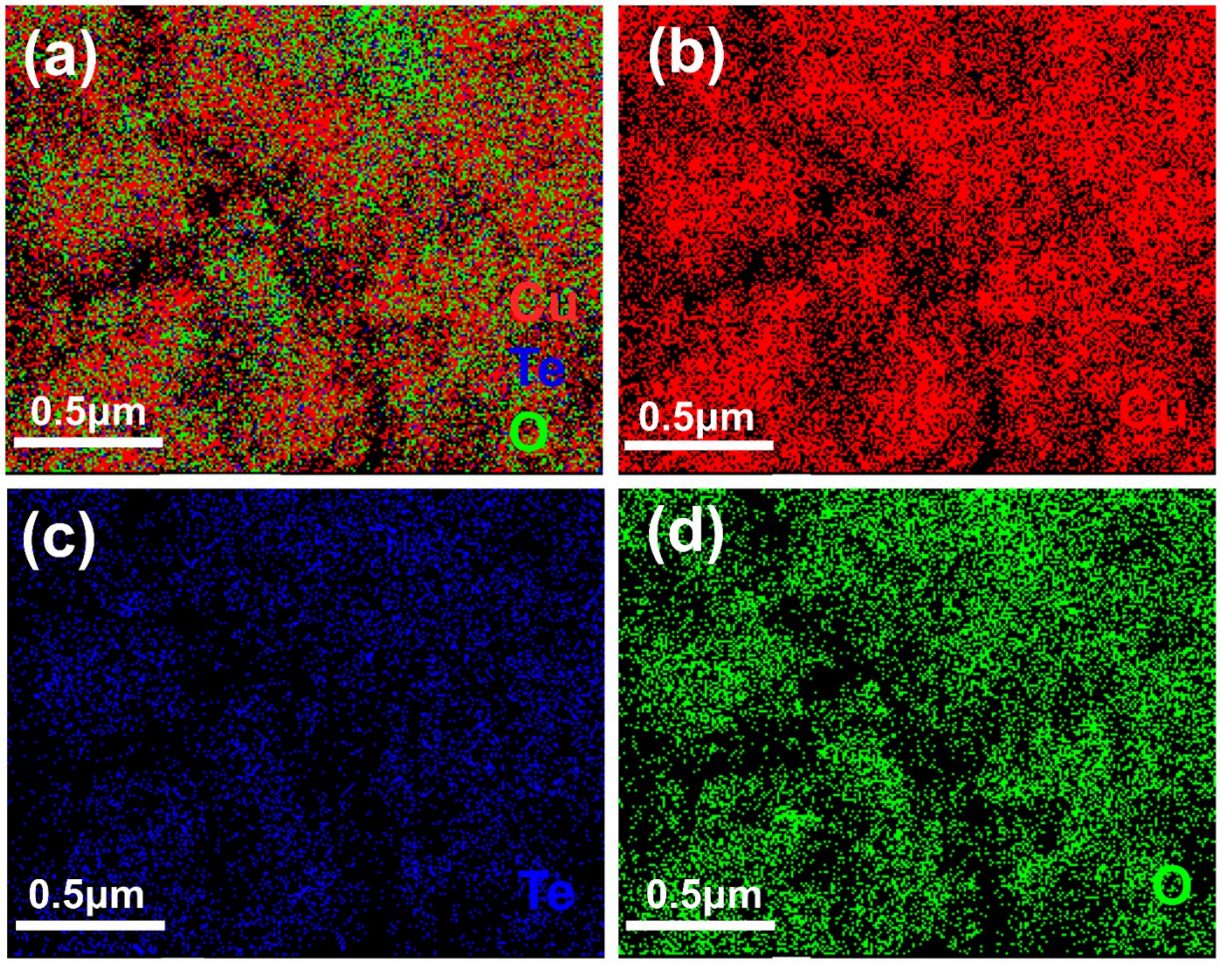

Fig. S3 (a) Combined elemental mapping of the $Cu_2O_8T_3$ NS and (b-d) elemental mapping of the individual Cu, Te, and O elements.

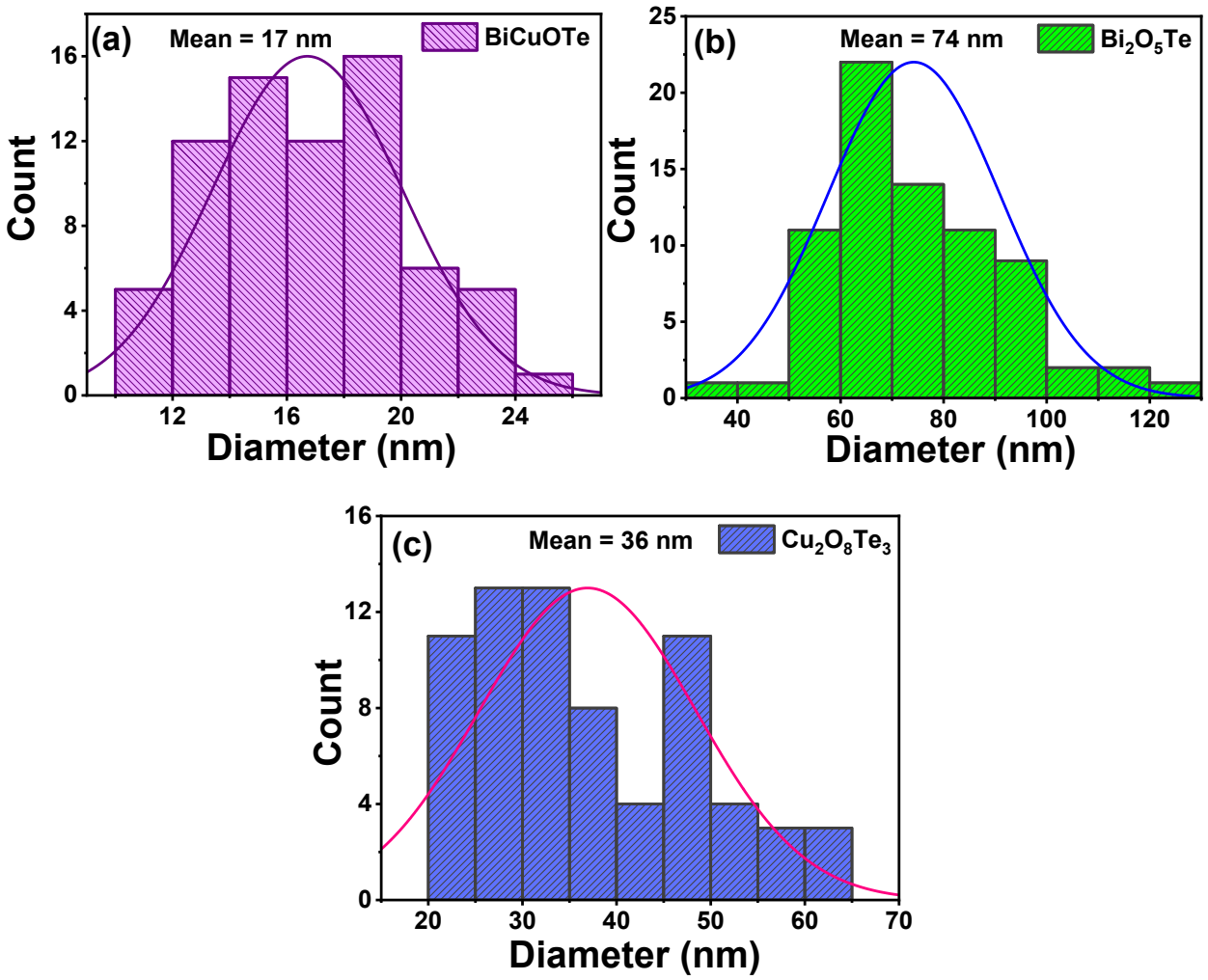

Fig. S4 Particle size distribution histogram of (a) BiCuOTe, (b) Bi_2O_5Te, and (c) $Cu_2O_8Te_3$ samples.

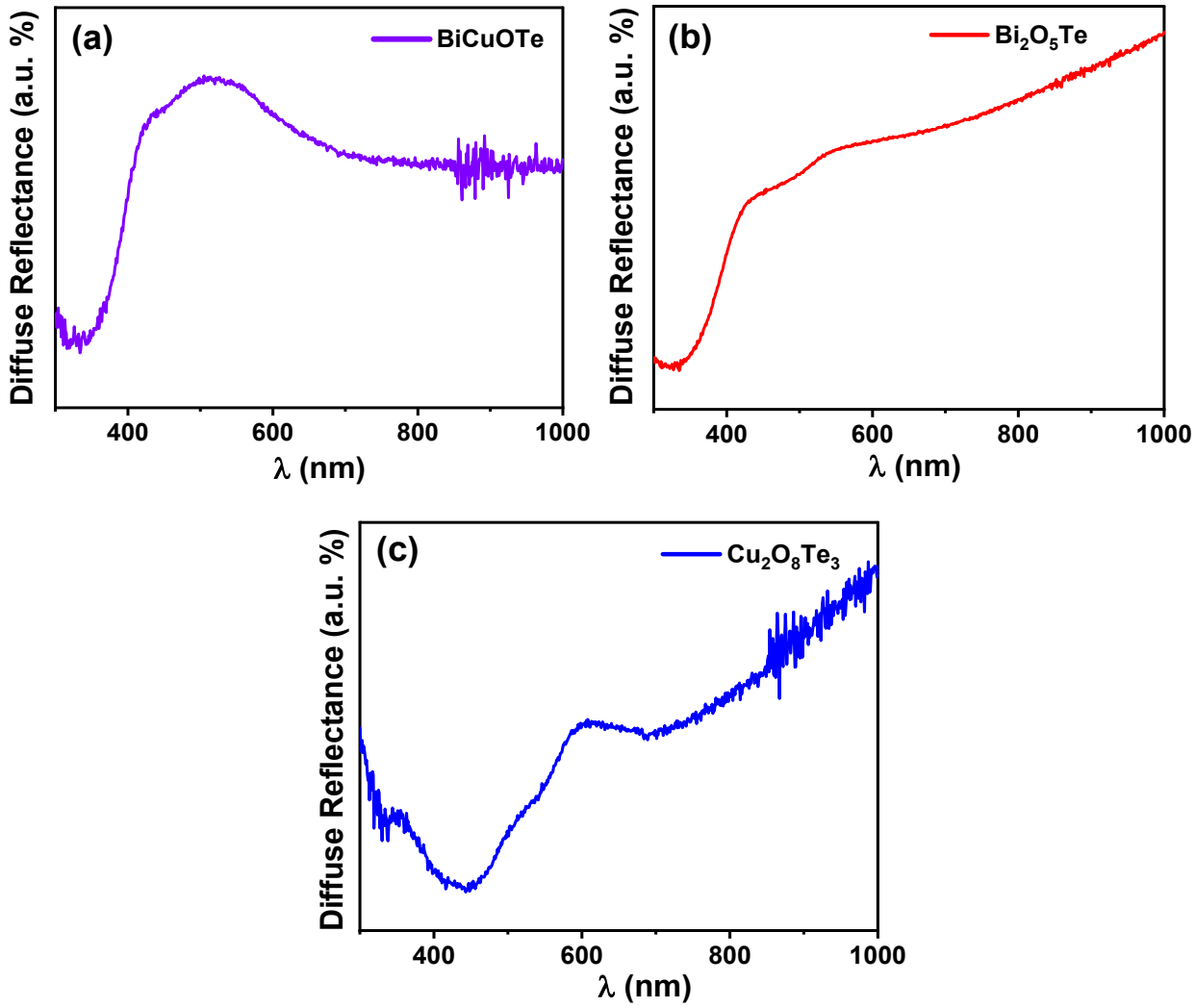

Fig. S5 Diffuse reflectance spectra of (a) BiCuOTe, (b) Bi_2O_5Te, and (c) $Cu_2O_8Te_3$ powder sample.

Table S1 Structural parameters obtained from XRD peak analysis.

Samples	Average Crystallite Size (D) (nm)	Dislocation density(δ) (nm^2)	Lattice Strain (ε)
BiCuOTe	20.36	0.00347	0.00539
Bi_2O_5Te	20.18	0.00537	0.00539
$Cu_2O_8Te_3$	13.98	0.00560	0.00735

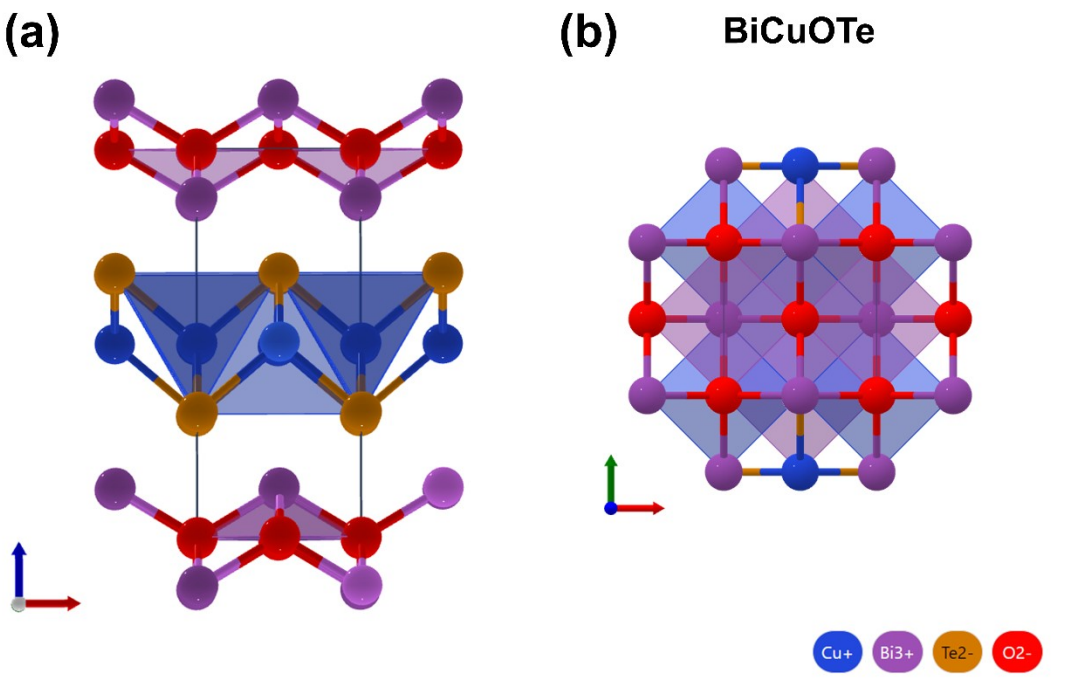

Fig. S6 Atomic configuration of BiCuOTe tetragonal crystal lattice system (a) side view and (b) top view with P4/nmm space group where the solid-line box shows the unit cell.[1]

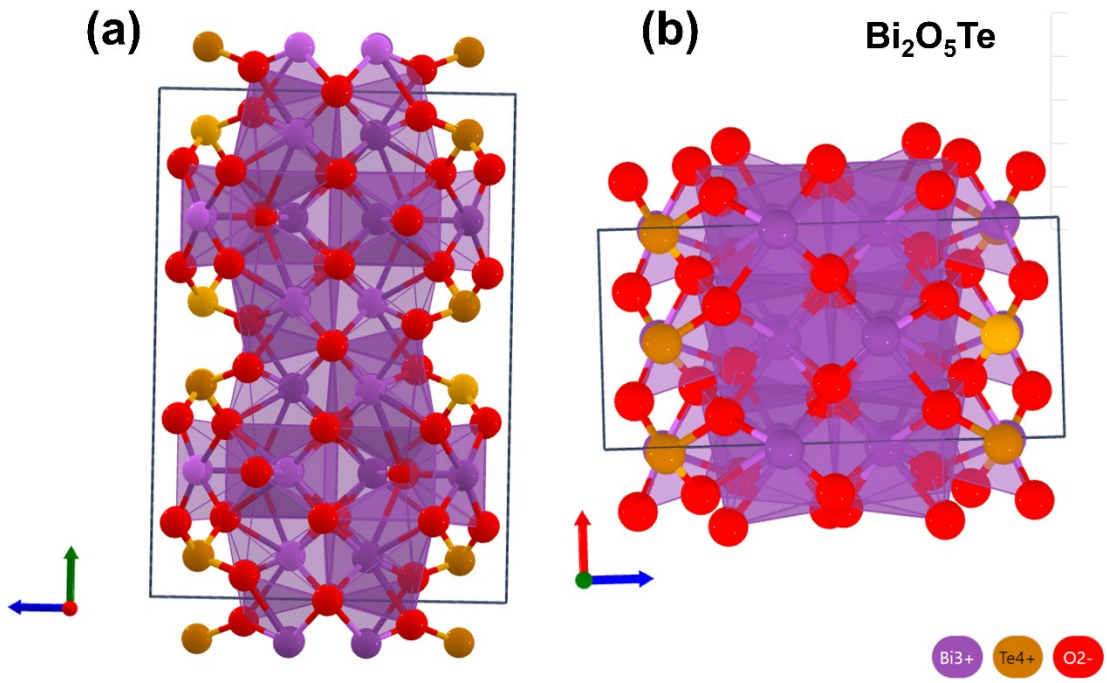

Fig. S7 Atomic configuration of Bi_2O_5Te orthorhombic lattice phase (a) side view and (b) top view with Aem2 space group where the unit cell is represented in solid-line box.[2]

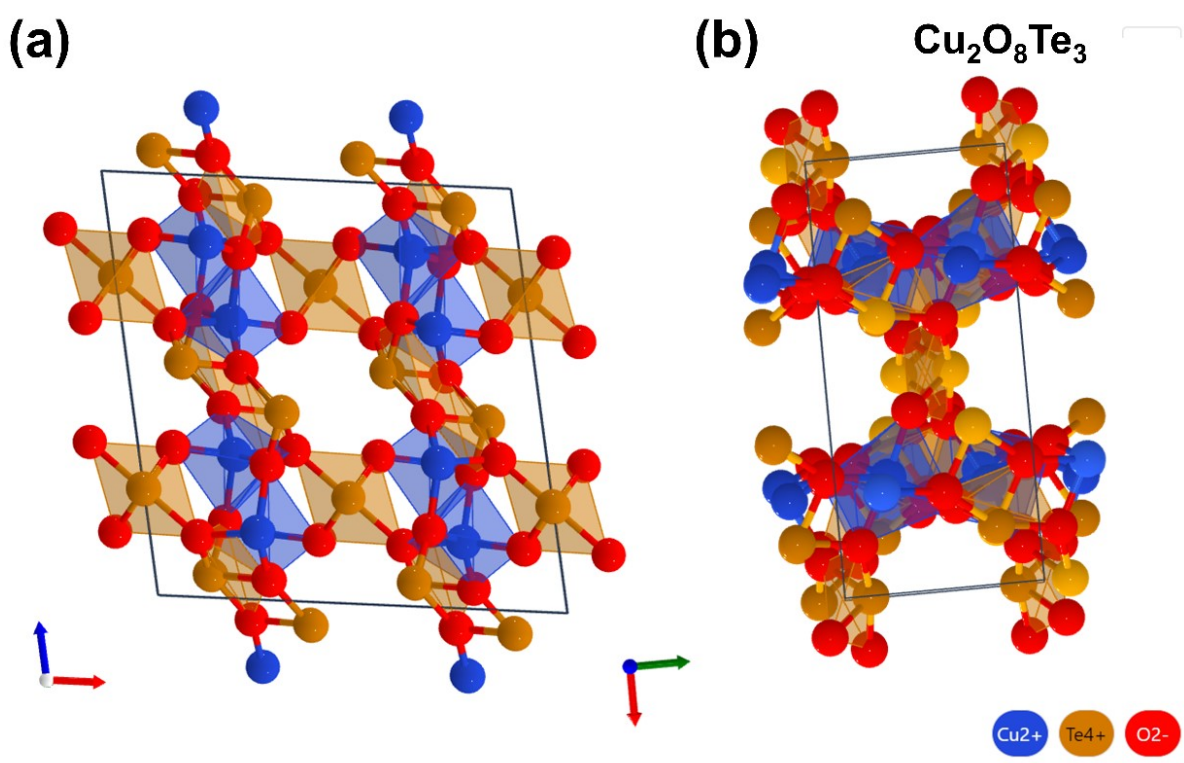

Fig. S8 Atomic configuration of $Cu_2O_8Te_3$ monoclinic crystal lattice system (a) side view and (b) top view with C2/c space group where the unit cell is exhibited by solid-line box.[3]

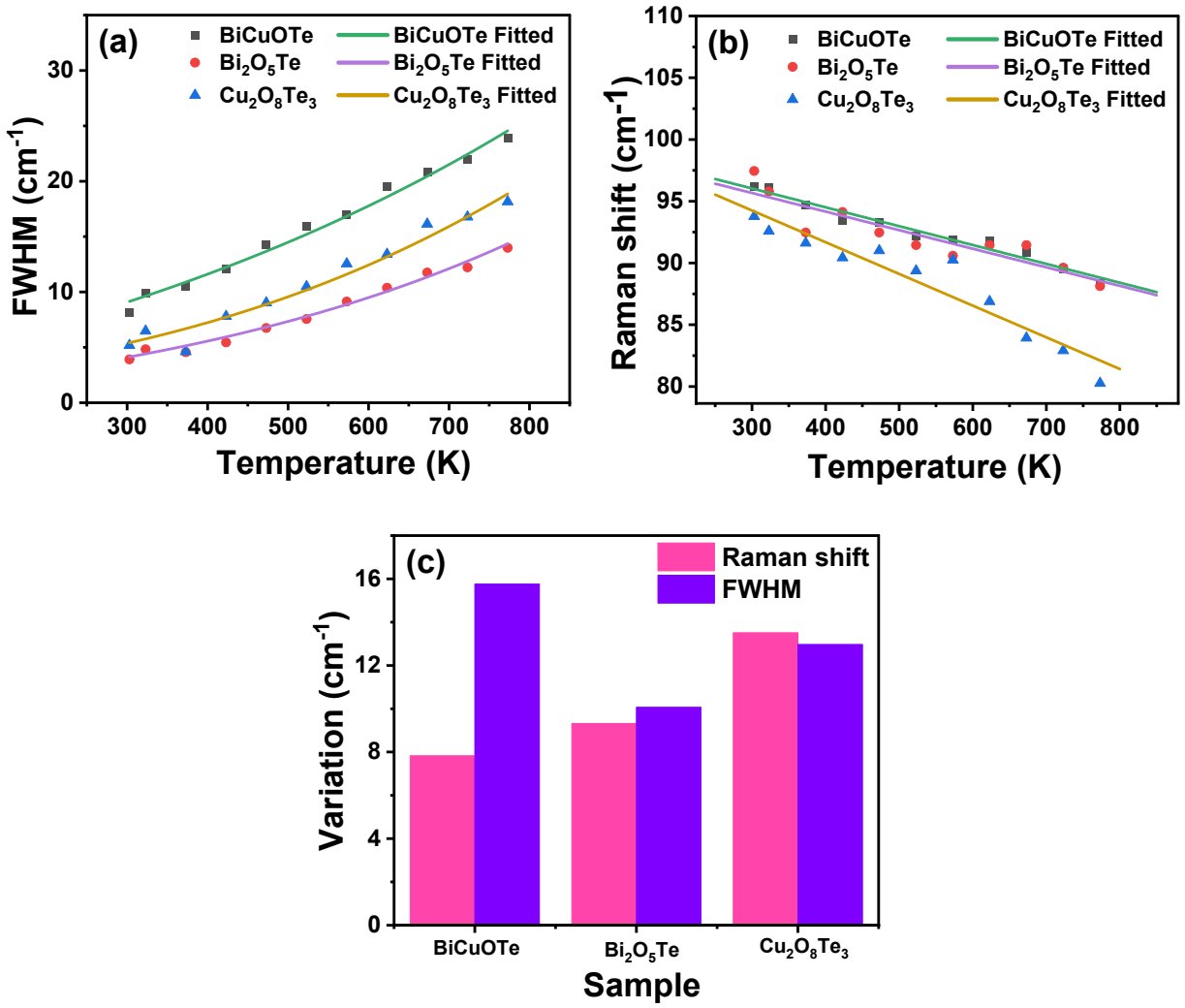

Fig. S9 Comparative plot between (a) FWHM of Raman peaks with respect to temperature, (b) Raman shift against temperature for Raman peaks appeared within 90~96 cm^{-1} and (c) statistical representation of the variation in Raman shift and FWHM of Raman peaks of each sample.

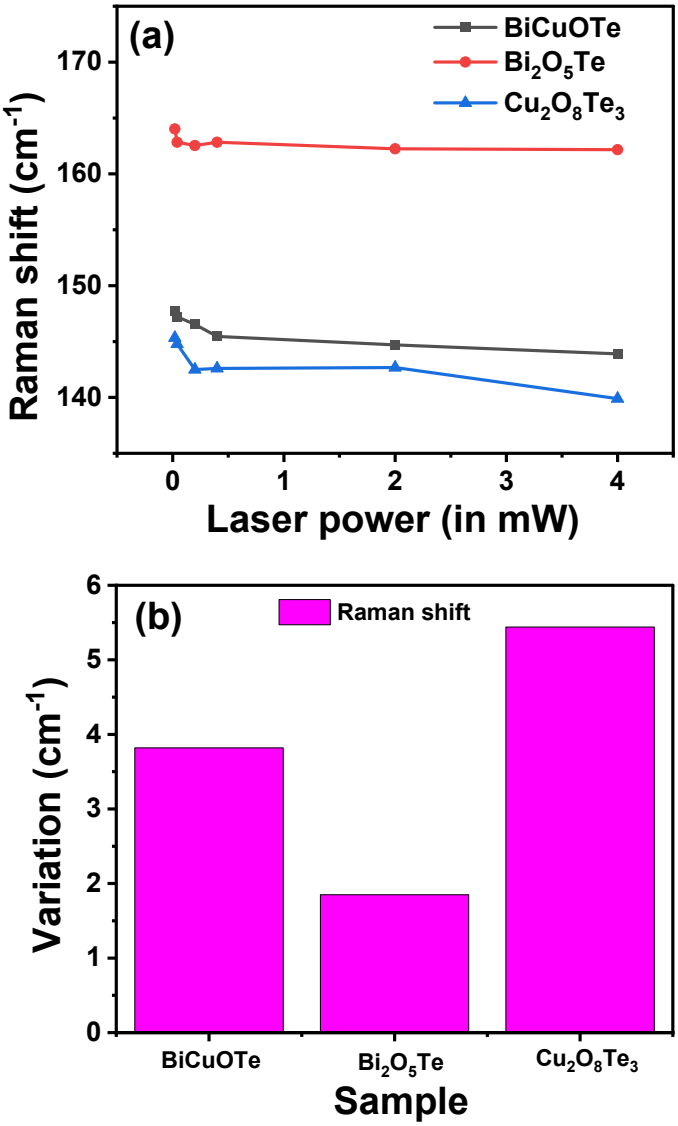

Fig. S10 Comparative plot between (a) Raman shift against laser power for Raman peaks that appeared within 145~164 cm^{-1} and (b) statistical representation of the variation in Raman shift of each sample.

Notes and references

1 *Data retrieved from the Materials Project for CuBiTeO (mp-545369) from database version v2023.11.1.*

2 *Data retrieved from the Materials Project for Bi_2TeO_5 (mp-23334) from database version v2023.11.1.*

3 *Data retrieved from the Materials Project for $Cu_2Te_3O_8$ (mp-17598) from database version v2023.11.1.*